12th International Symposium on Turbulence and Shear Flow Phenomena (TSFP12)
Osaka, Japan (Online), July 19-22, 2022

ON THE STREAMWISE WALL-SHEAR FLUCTUATIONS GENERATED BY ATTACHED EDDIES IN A TURBULENT CHANNEL FLOW

Cheng Cheng
Department of Mechanical and Aerospace Engineering
The Hong Kong University of Science and Technology
Clear Water Bay, Kowloon, Hong Kong
ccust@ust.hk

Lin Fu
Department of Mechanical and Aerospace Engineering
Department of Mathematics
Center for Ocean Research in Hong Kong and Macau (CORE)
The Hong Kong University of Science and Technology
Clear Water Bay, Kowloon, Hong Kong
Shenzhen Research Institute, The Hong Kong University of Science and Technology, Shenzhen, China
linfu@ust.hk

ABSTRACT

A growing number of studies suggest that the generation of wall-shear fluctuations is actively linked with the attached eddies populating the logarithmic region. In the present study, we investigate the statistical properties of the streamwise wall-shear fluctuations (τ_x') generated by attached eddies in a turbulent channel flow at $Re_\tau \approx 2000$. To this end, the superposition components of τ_x', which are correlated with logarithmic motions are identified by adopting an inner-outer predictive model. The momentum generation functions carried by them are calculated and compared with the scaling law predicted by the attached-eddy model. Our results further verify that the generation of τ_x' by attached eddies approximately follows an additive process.

INTRODUCTION

Wall-shear stress fluctuation is a crucial physical quantity in wall-bounded turbulence, as it is of importance for noise radiation, structural vibration, drag generation, and wall heat transfer, among others (Diaz-Daniel *et al.*, 2017; Cheng *et al.*, 2020). In the past two decades, ample evidence has shown that the root mean squared value of streamwise wall-shear stress fluctuations ($\tau_{x,rms}^{'}$) is sensitive to the flow Reynolds number (Abe *et al.*, 2004; Schlatter & Örlü, 2010; Yang & Lozano-Durán, 2017; Guerrero *et al.*, 2020). It indicates that large-scale energy-containing eddies populating the logarithmic and outer regions in high-Reynolds-number wall turbulence have non-negligible influences on the near-wall turbulence dynamics, and thus the wall friction (de Giovanetti *et al.*, 2016; Li *et al.*, 2019).

Till now, several models have been proposed on the organization of motions in logarithmic and outer regions and their interactions with the near-wall dynamics. Marusic *et al.* (2010) have established that superposition and modulation are the two basic mechanisms that large-scale motions (LSM) and very-large-scale motions (VLSM) exert influences on the near-wall turbulence. The former refers to the footprints of LSMs and VLSMs on the near-wall turbulence, while the latter indicates the intensity amplification or attenuation of near-wall small-scale turbulence by the outer motions. Mathis *et al.* (2013) extended the model to interpret the generation of wall-shear stress fluctuations in high-Reynolds number flows. They emphasized that superposition and modulation are still two essential factors. This inner-outer interaction model (IOIM) has also been successfully developed to predict the near-wall velocity fluctuations with data inputs from the log layer (Marusic *et al.*, 2010; Baars *et al.*, 2016; Wang *et al.*, 2021).

On the other hand, the most elegant conceptual model describing these energy-containing motions is the attached-eddy model (Townsend, 1976). It hypothesizes that the logarithmic region is occupied by an array of randomly-distributed and self-similar energy-containing motions (or eddies) with their roots attached to the near-wall region (see Fig. 1). During the recent decades, a growing body of evidence that supports the attached-eddy hypothesis has emerged rapidly, e.g., Hwang (2015), Hwang & Sung (2018), Hwang *et al.* (2020), to name a few. The reader is referred to a recent review work by Marusic & Monty (2019) for more details. Throughout the paper, the terms 'eddy' and 'motion' are exchangeable. It should be noted that the terms of 'wall-attached motions' and 'wall-attached eddies' used in the present study do not only refer to the self-similar eddies in the logarithmic region, but also the very-large-scale motions (VLSMs) or superstructures, as some recent studies have shown that VLSMs are also wall-attached, despite that their physical characteristics do not match the attached-eddy model (Hwang & Sung, 2018; Yoon *et al.*, 2020).

Previous study (Yang & Lozano-Durán, 2017) verified that the generation of wall-shear stress fluctuations can be interpreted as the outcomes of the momentum cascade across momentum-carried eddies of different scales, and modeled by

an additive process. Here, we first aim to couple the additive description with the AEM to portray the generation process of streamwise wall-shear fluctuations, resulting from wall-attached eddies. Then, we intend to isolate the streamwise wall-shear stress fluctuations generated by attached eddies in a turbulent channel flow at $Re_\tau = 2003$ ($Re_\tau = hu_\tau/\nu$, h denotes the channel half-height, u_τ the wall friction velocity and ν the kinematic viscosity) by resorting to the IOIM (Marusic *et al.*, 2010; Baars *et al.*, 2016). Direct comparison between the statistics from these two models will be conducted to verify the consistency.

DNS database and scale decomposition method

The DNS database adopted in the present study has been extensively validated by Jiménez and co-workers (Hoyas & Jiménez, 2006; Lozano-Durán & Jiménez, 2014*a*). The case at Re_τ=2003 is used and named as Re2000. The data are provided by the Polytechnic University of Madrid. Details of the parameter settings are listed in Table 1.

Table 1. Parameter settings of the DNS database. Here, L_x, L_y and L_z are the sizes of the computational domain in the streamwise, wall-normal and spanwise directions, respectively. N_F indicates the number of instantaneous flow fields used to accumulate statistics.

Case	Re_τ	$L_x(h)$	$L_y(h)$	$L_z(h)$	N_F
Re2000	2003	8π	2	3π	94

According to the inner-outer interaction model (Marusic *et al.*, 2010), the large-scale motions would exert the footprints on the near-wall region, i.e., the superposition effects. Baars *et al.* (2016) demonstrated that this component (denoted as $u_L^{'+}(x^+,y^+,z^+)$) can be obtained by the spectral stochastic estimation of the streamwise velocity fluctuation at the logarithmic region y_o^+, namely by

$$u_L^{'+}\left(x^+,y^+,z^+\right) = F_x^{-1}\left\{H_L\left(\lambda_x^+,y^+\right)F_x\left[u_o^{'+}\left(x^+,y_o^+,z^+\right)\right]\right\}, \tag{1}$$

where $u_o^{'+}$ is the streamwise velocity fluctuation at y_o^+ in the logarithmic region, and, F_x and F_x^{-1} denote the FFT and the inverse FFT in the streamwise direction, respectively. H_L is the transfer kernel, which evaluates the correlation between $u^{'+}(y^+)$ and $u_o^{'+}(y_o^+)$ at a given length scale λ_x^+, and can be calculated as

$$H_L\left(\lambda_x^+,y^+\right) = \frac{\left\langle \hat{u}'\left(\lambda_x^+,y^+,z^+\right)\overline{\hat{u}'}\left(\lambda_x^+,y_o^+,z^+\right)\right\rangle}{\left\langle \hat{u}'\left(\lambda_x^+,y_o^+,z^+\right)\overline{\hat{u}'}\left(\lambda_x^+,y_o^+,z^+\right)\right\rangle}, \tag{2}$$

where $\hat{u}'$ is the Fourier coefficient of u', and $\overline{\hat{u}'}$ is the complex conjugate of $\hat{u}'$.

In this paper, the main concern is the τ_x' generated by attached eddies populating logarithmic region. Thus, only the superposition term is taken into account. The predicted position y^+ is fixed at $y^+ = 0.3$, and y_0^+ varies from 100 (denoted as y_s^+, the lower bound of logarithmic region) to $0.2Re_\tau$ (denoted as y_e^+, the upper boundary of logarithmic region), i.e. the spanning of the logarithmic region (Jiménez, 2018). Once u_L is obtained, the streamwsie wall-shear fluctuation deduced by the superposition can be calculated by definition (i.e. $\nu\frac{\partial u_L}{\partial y}$ at the wall). We denote superposition component of $\tau_x^{'+}$ estimated from y_o^+ as $\tau_{x,L}^{'+}(y_o^+)$. According to the attached-eddy model, $\tau_{x,L}^{'+}(y_s^+) - \tau_{x,L}^{'+}(y_o^+)$ can be interpreted as the streamwsie wall-shear fluctuations generated by the wall-attached motions with wall-normal heights within y_s^+ and y_o^+, see Fig. 1.

Scaling law predicted by attached-eddy model

According to Yang & Lozano-Durán (2017), the wall-stress fluctuation can be modeled as an additive process. Similarly, the streamwise wall-shear fluctuations generated by attached eddies within y_o and y_s can be viewed as an discrete random contributions:

$$\tau_{x,a}^{'+} = \sum_{i=1}^{n} a_i, \tag{3}$$

where a_i are random additives, assumed to be identically and independently distributed (i.i.d), representing $\tau_x^{'+}$ associated with attached eddies at a given wall-normal height. The number of addends is $n \propto \int \frac{1}{y}dy \propto \ln(y_o/y_s)$. The momentum generation function $\left\langle exp(q\tau_{x,a}^{'+})\right\rangle$ can be evaluated as

$$\left\langle exp(q\tau_{x,a}^{'+})\right\rangle = \langle exp(qa)\rangle^{N_z} \sim (\frac{y_o}{y_s})^{\tau_q}, \tag{4}$$

where q is a real number, $\tau(q) = C_1 \ln\langle exp(qa)\rangle$ is called anomalous exponent, C_1 is an constant. (4) is called strong self similarity (SSS). If a is a Gaussian variable, the anomalous exponent can be recast as

$$\tau(q) = C_2 q^2, \tag{5}$$

where C_2 is an another constant. On the other hand, an extended self-similarity (ESS) is defined to describe the relationship between $\left\langle exp(q\tau_{x,o}^{'+})\right\rangle$ and $\left\langle exp(q_0\tau_{x,o}^{'+})\right\rangle$ (fixed q_0) (Benzi *et al.*, 1993), i.e.,

$$\left\langle exp(q\tau_{x,o}^{'+})\right\rangle = \left\langle exp(q_0\tau_{x,o}^{'+})\right\rangle^{\xi(q,q_0)}, \tag{6}$$

where $\xi(q,q_0)$ is a function of q (fixed q_0). Note that ESS does not strictly rely on i.i.d of the addends, but the additive process Eq. (3).

Considering that y_s^+ is the lower bound of the logarithmic region, the increase of y_o^+ in Eqs. (1) corresponds to the enlargement of the addends in the additive description (see Eq. (3)). In this way, the connection between AEM and IOIM are established, and the AEM predictions (see Eqs. (4)-(6)) can be verified directly.

Results and Discussion

To shed light on the generation mechanism of τ_x' associated with attached eddy, we define a moment generating function based on the above-mentioned decomposition, i.e.

$$G(q,y_o^+) = \left\langle exp(q(\tau_{x,L}^{'+}(y_s^+) - \tau_{x,L}^{'+}(y_o^+)))\right\rangle. \tag{7}$$

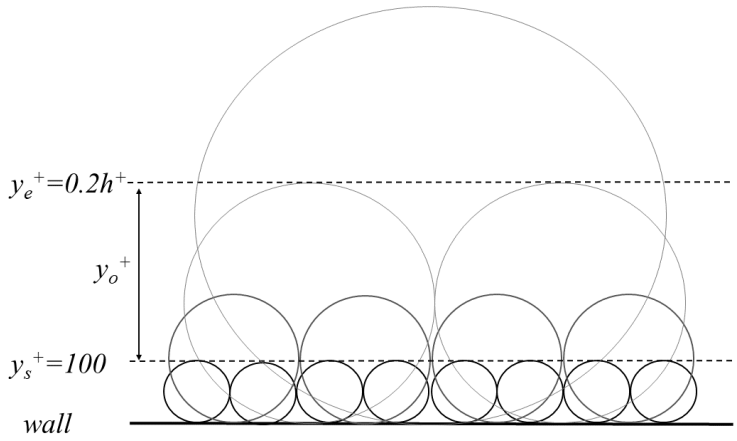

Figure 1. A schematic of the attached-eddy model (Hwang, 2015). Each circle represents an individual attached eddy. y_s^+ and y_e^+ are the lower and upper bound of the logarithmic region, respectively. y_0^+ is the outer reference height, and varies from y_s^+ to y_e^+.

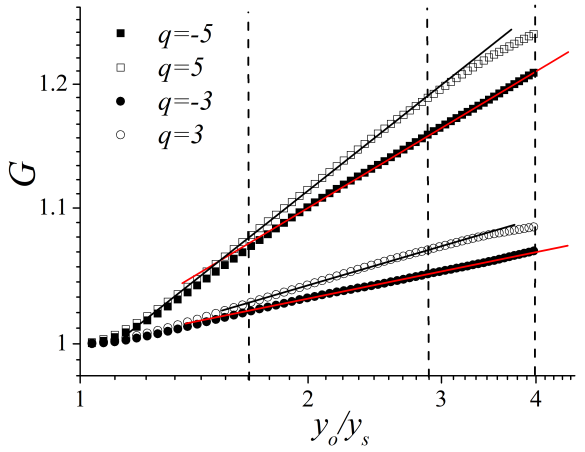

Figure 2. G as functions of y_o/y_s for $q=\pm5$ and $q=\pm3$.

Fig. 2 shows the variations of G as a function of y_o/y_s for $q=\pm5$ and $q=\pm3$. Power-law behaviours can be found in the interval between $1.7\leq y_o/y_s\leq 2.9$ for positive q and $1.7\leq y_o/y_s\leq 4$ for negative q, justifying the validity of SSS, i.e., Eq. (4). This observation highlights that the superpositions of wall-attached log-region motions on wall surface follow the additive process, characterized by Eq. (3). It is also worth mentioning that the power-law behaviour can be observed for larger wall-normal intervals for negative q. As $G(q,y_o^+)$ quantifies $\tau'^+_{x,L}(y_s^+)-\tau'^+_{x,L}(y_o^+)$, which features the same sign as q, this observation is consistent with the work of Cheng *et al.* (2020), which showed that the footprints of the inactive part of attached eddies populating the logarithmic region are actively connected with large-scale negative τ'_x. Other q values yield similar results and are not shown here for brevity.

The anomalous exponent $s(q)$ can be obtained by fitting the range $2\leq y_o/y_s\leq 2.9$, where both positive and negative q display good power-law scalings. Fig. 3(*a*) displays the variation of the anomalous exponent $s(q)$ as a function of q. The solid line denotes the quadratic fit within $-0.5\leq q\leq 0.5$. It can be seen that the variation of $s(q)$ is very close to the model prediction, i.e., the quadratic function as Eq. (5) with $C_2=0.00629$. Only minor discrepancies between DNS data and model predictions can be observed. As such, it is reasonable to hypothesize that the streamwise wall-shear stress fluctuation τ'_x generated by attached eddies of a given size follows

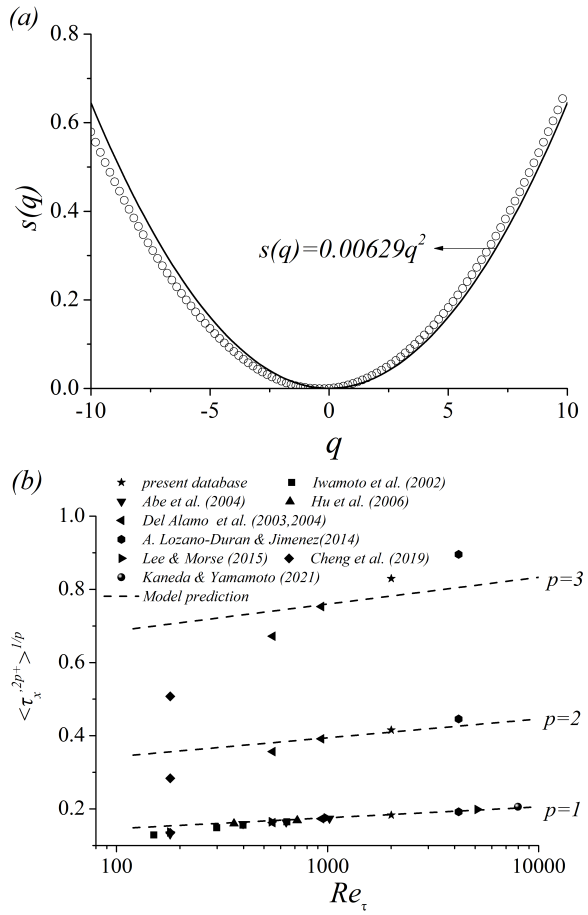

Figure 3. (*a*) Anomalous exponent $s(q)$ as a function of q. The black line is a quadratic fit; (*b*) second- to sixth- order moments of $\tau_x'^+$ as functions of Re_τ. The dashed lines are the log-normal predictions from Eq. (8)-(10).

the Gaussian distribution. Moreover, we can also estimate the statistical moments of $\tau^+_{x,o}$ by taking the derivative of $G(q,y_e^+)$ with respect to q around $q=0$ (Yang *et al.*, 2016), i.e.,

$$\left\langle \tau'^{2+}_{x,o}\right\rangle = \left.\frac{\partial^2 G(q;y_o^+)}{\partial q^2}\right|_{q=0} \sim 2C_2\ln Re_\tau, \qquad (8)$$

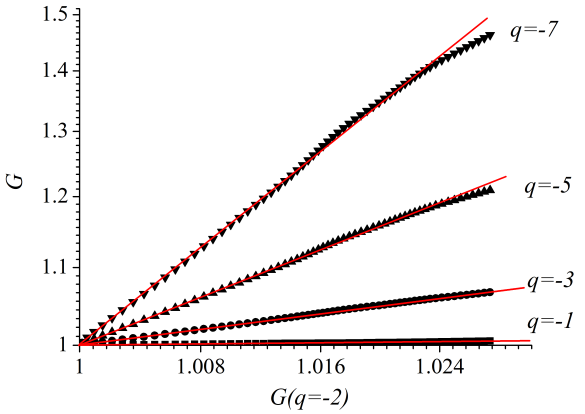

Figure 4. $G(q)$ as functions of $G(-2)$ for $q = -1,-3,-5,-7$. Both vertical and horizontal axes in (a) are plotted in logarithmic form.

$$\left\langle \tau_{x,o}^{\prime 4+} \right\rangle^{1/2} = \left(\frac{\partial^4 G(q;y_o^+)}{\partial q^4}\bigg|_{q=0} \right)^{1/2} \sim 2\sqrt{3}C_2 \ln Re_\tau, \quad (9)$$

$$\left\langle \tau_{x,o}^{\prime 6+} \right\rangle^{1/3} = \left(\frac{\partial^6 G(q;y_o^+)}{\partial q^6}\bigg|_{q=0} \right)^{1/3} \sim 2\sqrt[3]{15}C_2 \ln Re_\tau. \quad (10)$$

Fig. 3(b) shows the variations of second- ($p = 1$) to sixth- ($p = 3$) order moments of τ_x' calculated from DNS of channel flows (Iwamoto *et al.*, 2002; Del Álamo & Jiménez, 2003; Abe *et al.*, 2004; Del Álamo *et al.*, 2004; Hu *et al.*, 2006; Lozano-Durán & Jiménez, 2014*b*; Lee & Moser, 2015; Cheng *et al.*, 2019; Kaneda & Yamamoto, 2021) and compares them with the model prediction, i.e., Eq. (8)-(10). For the second- and fourth- order variances, the model predictions are roughly consistent with the DNS results. The comparisons also indicate a Reynolds-number dependence of $\left\langle \tau_x^{\prime 2+} \right\rangle$, which has been reported by vast studies (Schlatter & Örlü, 2010; Mathis *et al.*, 2013; Guerrero *et al.*, 2020), and may be ascribed to the superposition effects of the wall-attached log-region motions. For sixth-order moments, the model prediction displays substantial discrepancies with the DNS data. It is expected since high-order moments are dominated by the rare events resulting from the intermittent small-scale motions (Frisch & Donnelly, 1996), which can not be captured by IOIM.

ESS (i.e., Eq. (6)) is another scaling predicted by the multifractal formalism. Different from SSS, ESS does not rely on the i.i.d of the addends, but the additive process (see Eq. (3)). Fig. 4 shows the ESS scalings for $q_0 = -2$ and $q_0 = 2$, respectively. ESS holds for the entire logarithmic region. The observation suggests that the streamwise wall-shear fluctuations generated by logarithmic motions obey the additive process, though the streamwise wall shear fluctuations generated by attached eddies with wall-normal heights at approximately $0.2h^+$ are not identically and independently distributed due to the scale interactions (see Fig. 2), which are not described by the attached-eddy model.

CONCLUSIONS

In summary, the present study reveals that IOIM and AEM are consistent to each other quantitatively. The statistical characteristics of the superpositions of log-region eddies follow the predictions of AEM, namely, the SSS and ESS scalings. Based on these observations, we conclude that the streamwise wall-shear stress fluctuations generated by attached eddies populating the logarithmic region can be treated as Gaussian variables. Considering the fact that the intensity of wall-shear stress fluctuations is typically underpredicted by the state-of-the-art wall-modelled large-eddy simulation (WMLES) approaches (Park & Moin, 2016), the results proposed in the present study may be constructive for the development of the LES methodology.

ACKNOWLEDGMENT

We are grateful to the authors cited in Fig. 3(b) for making their invaluable data available. Lin Fu has been founded by the fund from Guangdong Basic and Applied Basic Research Foundation (No. 2022A1515011779), the fund from CORE as a joint research center for ocean research between QNLM and HKUST, and the fund from Shenzhen Municipal Central Government Guides Local Science and Technology Development Special Funds Funded Projects (NO. 2021Szvup138).

REFERENCES

Abe, H., Kawamura, H. & Choi, H. 2004 Very large-scale structures and their effects on the wall shear-stress fluctuations in a turbulent channel flow up to $Re_\tau = 640$. *J. Fluids Eng.* **126** (5), 835–843.

Baars, W. J, Hutchins, N. & Marusic, I. 2016 Spectral stochastic estimation of high-reynolds-number wall-bounded turbulence for a refined inner-outer interaction model. *Physical Review Fluids* **1** (5), 054406.

Benzi, R., Ciliberto, S., Tripiccione, R., Baudet, C., Massaioli, F. & Succi, S. 1993 Extended self-similarity in turbulent flows. *Phys. Rev. E* **48**, R29–R32.

Blackman, K., Perret, L. & Mathis, R. 2019 Assessment of inner–outer interactions in the urban boundary layer using a predictive model. *J. Fluid Mech.* **875**, 44–70.

Cheng, C., Li, W., Lozano-Durán, A. & Liu, H. 2019 Identity of attached eddies in turbulent channel flows with bidimensional empirical mode decomposition. *J. Fluid Mech* **870**, 1037–1071.

Cheng, C., Li, W., Lozano-Durán, A. & Liu, H. 2020 On the structure of streamwise wall-shear stress fluctuations in turbulent channel flows. *J. Fluid Mech.* **903**, A29.

Del Álamo, J. C. & Jiménez, J. 2003 Spectra of the very large anisotropic scales in turbulent channels. *Phys. Fluids* **15** (6), L41–L44.

Del Álamo, J. C., Jiménez, J., Zandonade, P. & Moser, R.D. 2004 Scaling of the energy spectra of turbulent channels. *J. Fluid Mech.* **500**, 135–144.

Diaz-Daniel, C., Laizet, S. & Vassilicos, J.C. 2017 Wall shear stress fluctuations: Mixed scaling and their effects on velocity fluctuations in a turbulent boundary layer. *Phys. Fluids* **29** (5), 055102.

Frisch, U. & Donnelly, R.J. 1996 *Turbulence: the legacy of AN Kolmogorov*. AIP.

de Giovanetti, M., Hwang, Y. & Choi, H. 2016 Skin-friction generation by attached eddies in turbulent channel flow. *J. Fluid Mech.* **808**, 511–538.

Guerrero, B., Lambert, M.F. & Chin, R.C. 2020 Extreme wall shear stress events in turbulent pipe flows: spatial characteristics of coherent motions. *J. Fluid Mech.* **904**, A18.

Hoyas, S. & Jiménez, J. 2006 Scaling of the velocity fluctuations in turbulent channels up to $Re_\tau = 2003$. *Phys. Fluids* **18** (1), 011702.

Hu, Z.W., Morfey, C.L. & Sandham, N.D. 2006 Wall pressure and shear stress spectra from direct simulations of channel flow. *AIAA Journal* **44** (7), 1541–1549.

Hwang, J., Lee, J. & Sung, H. 2020 Statistical behaviour of self-similar structures in canonical wall turbulence. *J. Fluid Mech.* **905**, A6.

Hwang, J. & Sung, H.J. 2018 Wall-attached structures of velocity fluctuations in a turbulent boundary layer. *J. Fluid Mech.* **856**, 958–983.

Hwang, Y. 2015 Statistical structure of self-sustaining attached eddies in turbulent channel flow. *J. Fluid Mech.* **767**, 254–289.

Iwamoto, K., Suzuki, Y. & Kasagi, N. 2002 Reynolds number effect on wall turbulence: toward effective feedback control. *Int. J. Heat Fluid Flow* **23** (5), 678–689.

Jiménez, J. 2018 Coherent structures in wall-bounded turbulence. *J. Fluid Mech.* **842**, P1.

Kaneda, Y. & Yamamoto, Y. 2021 Velocity gradient statistics in turbulent shear flow: an extension of kolmogorov's local equilibrium theory. *J. Fluid Mech.* **929**, A13.

Lee, M. & Moser, R.D. 2015 Direct numerical simulation of turbulent channel flow up to $Re_\tau \approx 5200$. *J. Fluid Mech.* **774**, 395–415.

Li, W., Fan, Y., Modesti, D. & Cheng, C. 2019 Decomposition of the mean skin-friction drag in compressible turbulent channel flows. *J. Fluid Mech.* **875**, 101–123.

Lozano-Durán, A. & Jiménez, J. 2014*a* Effect of the computational domain on direct simulations of turbulent channels up to $Re_\tau = 4200$. *Phys. Fluids* **26** (1), 011702.

Lozano-Durán, A. & Jiménez, J. 2014*b* Time-resolved evolution of coherent structures in turbulent channels: characterization of eddies and cascades. *J. Fluid Mech.* **759**, 432–471.

Marusic, I., Mathis, R. & Hutchins, N. 2010 Predictive model for wall-bounded turbulent flow. *Science* **329** (5988), 193–196.

Marusic, I. & Monty, J.P. 2019 Attached eddy model of wall turbulence. *Annu. Rev. Fluid Mech.* **51**, 49–74.

Mathis, R., Hutchins, N. & Marusic, I. 2011 A predictive inner–outer model for streamwise turbulence statistics in wall-bounded flows. *J. Fluid Mech.* **681**, 537–566.

Mathis, R., Marusic, I., Chernyshenko, S.I. & Hutchins, N. 2013 Estimating wall-shear-stress fluctuations given an outer region input. *J. Fluid Mech.* **715**, 163–180.

Park, G.I. & Moin, P. 2016 Space-time characteristics of wall-pressure and wall shear-stress fluctuations in wall-modeled large eddy simulation. *Phys. Rev. Fluids* **1** (2), 024404.

Schlatter, P. & Örlü, R. 2010 Assessment of direct numerical simulation data of turbulent boundary layers. *J. Fluid Mech.* **659**, 116–126.

Townsend, A. A. 1976 *The structure of turbulent shear flow*, 2nd edn. Cambridge University Press.

Wang, J., Pan, C. & Wang, J. 2020 Characteristics of fluctuating wall-shear stress in a turbulent boundary layer at low-to-moderate Reynolds number. *Phys. Rev. Fluids* **5** (7), 074605.

Wang, L., Hu, R. & Zheng, X. 2021 A scaling improved inner–outer decomposition of near-wall turbulent motions. *Physics of Fluids* **33** (4), 045120.

Yang, X.I.A. & Lozano-Durán, A. 2017 A multifractal model for the momentum transfer process in wall-bounded flows. *J. Fluid Mech.* **824**, R2.

Yang, X.I.A., Marusic, I. & Meneveau, C. 2016 Moment generating functions and scaling laws in the inertial layer of turbulent wall-bounded flows. *J Fluid Mech* **791**, R2.

Yoon, M., Hwang, J., Yang, J. & Sung, H.J. 2020 Wall-attached structures of streamwise velocity fluctuations in an adverse-pressure-gradient turbulent boundary layer. *J. Fluid Mech.* **885**, A12.